I&EC research
Industrial & Engineering Chemistry Research

Article

Cite This: Ind. Eng. Chem. Res. 2018, 57, 14242−14253

pubs.acs.org/IECR

Toluene/*n*-Heptane Separation by Extractive Distillation with Tricyanomethanide-Based Ionic Liquids: Experimental and CPA EoS Modeling

Pablo Navarro,*[,†] Miguel Ayuso,[‡] André M. Palma,[†] Marcos Larriba,[†,‡] Noemí Delgado-Mellado,[‡] Julián García,[‡] Francisco Rodríguez,[‡] João A. P. Coutinho,[†] and Pedro J. Carvalho[†]

[†]CICECO − Aveiro Institute of Materials, Department of Chemistry, University of Aveiro, Aveiro 3810-193, Portugal

[‡]Department of Chemical Engineering, Complutense University of Madrid, Madrid E−28040, Spain

Supporting Information

ABSTRACT: This work covers the phase equilibrium characterization of systems containing *n*-heptane, toluene, and two tricyanomethanide-based ionic liquids (ILs), 1-ethyl-3-methylimidazolium tricyanomethanide ([C_2C_1im][TCM]) and 1-butyl-4-methylpyridinium tricyanomethanide ([4-C_4C_1py][TCM]). Aiming at evaluating these ILs for the *n*-heptane/toluene extractive distillation, the vapor−liquid−liquid equilibria (VLLE) and vapor−liquid equilibria (VLE) were determined by headspace-gas chromatography (HS-GC) in the whole composition range at temperatures from 323.2 to 423.2 K and solvent to feed (S/F) ratios of 1, 5, and 10. Experimental results were modeled with the Cubic Plus Association (CPA) Equation of State (EoS). ILs' molecular parameters were regressed through density and heat capacity data and further used to describe the binary and ternary mixtures phase equilibria. Extractive distillation with ILs stands as a powerful approach for the dearomatization of liquid fuels, whereas the combination of HS-GC methodology and CPA EoS has been revealed as an ideal strategy to further exploring this new technology.

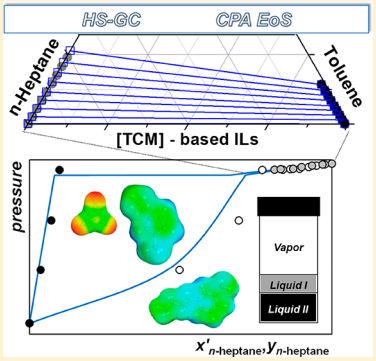

1. INTRODUCTION

The separation of compounds with close boiling points is one of the most relevant challenges in the oil industry. Accordingly, the design of new separation processes using new configurations and solvents stands as an important issue to enable better technologies and increase purity standards. Among all separations in the oil industry, the aromatic separation from refinery streams, that is, reformer and pyrolysis gasolines, is one of the most challenging due to the close boiling points of the compounds in these streams, which translates into high energy demanding steps in current-technologies based on volatile organic compounds such as sulfolane.[1]

Aromatic/aliphatic separation using ionic liquids (ILs) has received special attention by the research community aiming at developing more efficient processes with lower environmental impact at milder conditions.[2] ILs are considered designer solvents due to the wide variety of species that can be synthesized through their anion and cation combinations.[3] Furthermore, the ILs' design can be tuned aiming at achieving desirable properties for specific separations or applications. Additionally, ILs present outstanding properties that provide an advantage when compared to other conventional solvents, like negligible vapor pressures and wide liquid ranges, the latter due to their low melting points,[4] and relatively high thermal stability.[5]

The development of the aromatic/aliphatic separation by liquid−liquid extraction using ILs has been proved technically feasible, although several limitations, regarding operating costs, have been identified.[6−10] The extractor inability to separate and purify aromatics and aliphatics demands further separation and purification steps at low vacuum conditions.[9,10] The use of an extractive distillation configuration, instead of a liquid−liquid extraction, allows one to separate and purify aromatics and aliphatics with proven advantages.[11]

Extractive distillation using ILs stands out as an alternative to the liquid−liquid extraction with improved aromatic/aliphatic separation[11−17] because of the feasibility of achieving specifications with a single separation unit[18] and no solvent losses (negligible vapor pressure of ILs[11]). Furthermore, the only additional separation required is that of the aromatic/IL separation for the residue stream, but a simple flash distillation unit, operating under vacuum conditions, or a stripping column can be envisioned.[9,18−20]

In a recent work, the transferability between these two technologies has been explored. ILs were screened aiming at maximizing the extractive properties (capacity or/and selectivity), the solvent thermal stability, and minimizing the viscosity. As reported, the IL capacity stands as the main enhancer for the *n*-heptane/toluene relative volatility for heterogeneous extractive distillation, whereas selectivity had the leading role for

Received: August 10, 2018
Revised: September 24, 2018
Accepted: September 28, 2018
Published: September 28, 2018

DOI: 10.1021/acs.iecr.8b03804
Ind. Eng. Chem. Res. 2018, 57, 14242−14253

homogeneous extractive distillation. Furthermore, the temperature has an important impact on the vapor/liquid distribution, with low temperatures establishing high capacity mass agents as the best candidates and the opposite trend observed for high temperatures.[21]

Tricyanomethanide-based ILs were previously reported, within the 323.2−403.2 K temperature range, as the most efficient entrainers, leading to the highest *n*-heptane/toluene mean relative volatility, high thermal stability (round 450 K for long-term scenarios), and the lowest viscosities among all of the studied ILs.[2,22−24]

In this work, the VLE and/or VLLE was evaluated for binary and ternary systems in the whole hydrocarbon composition range for the ionic liquids 1-ethyl-3-methylimidazolium tricyanomethanide, $[C_2C_1im][TCM]$, and 1-butyl-4-methylpyridinium tricyanomethanide, $[4\text{-}C_4C_1py][TCM]$, at temperatures ranging from 323.2 to 423.2 K, exploring S/F ratios of 1, 5, and 10 on the ternary systems. Experimental data were determined by HS-GC methodology, and the CPA EoS was selected as a suitable EoS to describe the phase equilibria of the systems. To obtain a proper selection of a coarse-grained model capable of representing most of the physical features of the compounds, density (ρ) and heat capacity (C_p) at 0.1 MPa were used to independently determine the ILs' molecular parameters.

2. EXPERIMENTAL SECTION

2.1. Chemicals. The ILs 1-ethyl-3-methylimidazolium tricyanomethanide, $[C_2C_1im][TCM]$, and 1-butyl-4-methylpyridinium tricyanomethanide, $[4\text{-}C_4C_1py][TCM]$, were acquired from Iolitec GmbH with purities higher than 98 wt %. The ILs were further purified through a drying procedure under vacuum (50 Pa) and moderate temperature (313 K). Toluene and *n*-heptane were supplied by Sigma-Aldrich with purities higher than 99.5 wt % and were kept in their original vessels over 3 Å molecular sieves. Additional details for the chemicals used can be found in Table 1.

Table 1. Compound Description, Supplier, Water Content, Mass Fraction Purity, and Supplier of the Studied Compounds

chemical	supplier	purity in wt %	water content in ppm
$[C_2C_1im][TCM]$	Iolitec GmbH	98	<300
$[4\text{-}C_4C_1py][TCM]$	Iolitec GmbH	98	<300
n-heptane	Sigma-Aldrich	99.7	anhydrous
toluene	Sigma-Aldrich	99.5	anhydrous

2.2. Determination of VLE/VLLE. The VLLE and VLE data were determined by the HS-GC technique as fully detailed in previous works.[21,25] The mixtures were prepared by mass using a Mettler Toledo XS205 balance, with a precision of 10^{-5} g, in 20 mL sealed glass vials. Each mixture point was prepared in duplicate, and the phases were allowed to reach equilibrium for a period never smaller than 2 h. Equilibration time was experimentally checked to be lower than 2 h by monitoring the evolution of the peak areas with equilibrium time.

The vapor phase was sampled by an Agilent 7697A Headspace injector and analyzed with an Agilent 7890A GC. After equilibrium was achieved, the vapor phase was analyzed by GC using the response factor method to correct the compositions. For the mixtures presenting two phases, a liquid and a vapor phase, the liquid mole fractions (x_i) were determined by mass balance knowing the mixture point compositions (z_i) and the vapor phase composition:

$$x_i = \frac{z_i F - (p_i V_G/RT)}{\sum_{i=1}^{3}(z_i F - (p_i V_G/RT))} \quad (1)$$

where F denotes the molar amount of the feed, V_G is the headspace volume of the vial, and R is the ideal gas law constant. Partial pressures (p_i) of *n*-heptane and toluene were obtained together with the vapor phase composition using the relationship between the peak areas of the hydrocarbons (A_i) and the peak areas developed by each hydrocarbon alone in the same conditions (A_i^0):

$$p_i = \frac{p_i^0 A_i}{A_i^0} \quad (2)$$

where p_i^0 refers to the vapor pressure of each pure hydrocarbon, taken from the literature.[26] Thus, the total pressure was calculated as the sum of the partial pressures.

For the VLLE measurements, similar to the VLE experiments, the mixture points were prepared in duplicate, and the phases were allowed to reach equilibrium for a period never smaller than 2 h. The mixture gas phase was then sampled with the Agilent 7697A headspace injector and analyzed using the Agilent 7890A GC. The bottom liquid phase was sampled with an insulin syringe (BD Micro-Fine, 0.3 mL) and analyzed by multiple headspace extraction (MHE) technique. The details and background of the MHE method are widely explained in a previous work.[23] Knowing the compositions of the vapor and IL-rich liquid phase, the composition of the hydrocarbon-rich liquid phase was determined by mass balance.

2.3. Determination of Heat Capacity at Constant Pressure. The measurement of the heat capacity at constant pressure (C_p) for the $[4\text{-}C_4C_1py][TCM]$ IL was performed by differential scanning calorimetry using a Mettler Toledo DSC821e. A sample of 25 ± 1 mg was placed in triplicate into 40 μL stainless steel pans and under an inert atmosphere of nitrogen. The IL drying was done in situ to avoid the water impact on the measurements. Further details of the methodology can be found in a previous work.[24]

3. CPA EoS MODELING

Kontegeorgis et al.[27,28] proposed a simplified CPA EoS version combining the Soave−Redlich−Kwong (SRK) physical contribution[29,30] together with an association term originally theorized by Wertheim that incorporates intermolecular interaction, that is, hydrogen bonding and solvation, and is also frequently used in different association models (SAFT-type EoS).[31−33] The CPA EoS approach is expressed in terms of compressibility factor (Z) as follows:

$$Z = Z^{phys} + Z^{assoc} = \frac{1}{1-b\rho} - \frac{a\rho}{RT(1+b\rho)} - \frac{1}{2}\left(1 + \rho\frac{\ln \partial g}{\partial \rho}\right)\sum_i x_i \sum_i (1 - X_{Ai}) \quad (3)$$

where a and b are energy and covolume parameters, respectively, for the physical term, whereas g refers to a simplified hard-sphere radial distribution, and X_{Ai} is the mole fraction of component i not bonded at site A for the association contribution. The

DOI: 10.1021/acs.iecr.8b03804
Ind. Eng. Chem. Res. 2018, 57, 14242−14253

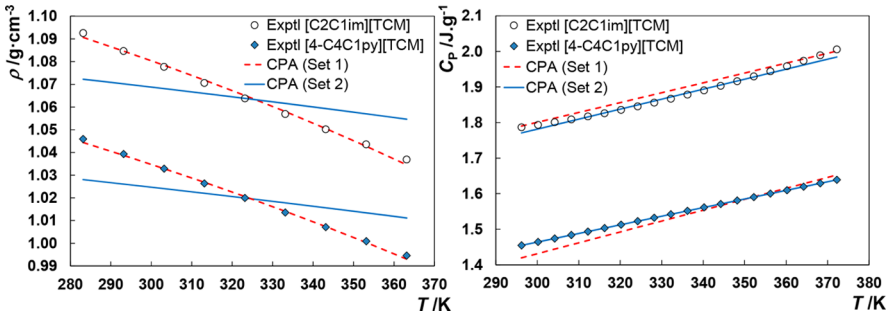

Figure 1. Density (ρ) and heat capacity (C_p) at 0.1 MPa as a function of temperature: experimental and CPA EoS modeling.

parameter a is given by a Soave-type temperature-dependent relation:[29]

$$a(T) = a_0[1 + c_1(1 - T_r^{0.5})]^2 \quad (4)$$

where a_0 and c_1, together with the temperature-independent b, are the three parameters needed to define nonassociation compounds. These parameters are regressed from the properties of the pure component. Here, the three parameters for *n*-heptane and toluene were taken from the literature where they were regressed from their vapor pressures and liquid densities.[34] The nonvolatility character of ILs makes the existence of vapor pressures and saturated liquid densities nonexistent. Thus, aiming to propose molecular parameters for the studied ILs with sound physical meaning, the CPA parameters were determined by regressing the EoS against atmospheric density and heat capacity data.

Regarding the association contribution, here explored for the ILs, X_{Ai} is mathematically related to the association strength (Δ^{AiBj}) between sites from two different molecules and is defined with the next set of equations:

$$X_{Ai} = \frac{1}{1 + \rho \sum_j x_j \sum_{Bj} X_{Bj} \Delta^{AiBj}} \quad (5)$$

$$\Delta^{AiBj} = g(\rho)\left[\exp\left(\frac{\varepsilon^{AiBj}}{RT}\right)a - 1\right]b_{ij}\beta^{AiBj} \quad (6)$$

$$g(\rho) = \frac{1}{1 - 1.9\eta}; \qquad \eta = \frac{1}{4}b\rho \quad (7)$$

where ε^{AiBj} and β^{AiBj} are the association energy and volume for a pure compound, respectively. These two association parameters are commonly regressed in the same way as explained before and together with the three cubic parameters comprise the required parameters for a pure association compound. To apply CPA EoS to experimental systems, a molecular model, able to represent the basic physical features of the compound, must be proposed. Although *n*-heptane and toluene are considered nonassociative compounds,[34] imidazolium-based ILs have been reported as associative compounds with two association sites (scheme 2B).[35−38] Furthermore, Oliveira et al.[37] reported that the alkyl chain length and the cation nature (pyridinium or imidazolium) showed no influence in the association scheme, while Maia et al.[38] proposed the same association scheme (scheme 2B) for other imidazolium-based ILs, 1-ethyl-3-methylimidazolium bis(trifluoromethylsulfonyl)imide and 1-butyl-3-methylimidazolium bis(trifluoromethylsulfonyl)imide, in their modeling using the CPA EoS; on the basis of these works, the 2B scheme was adopted for the ILs evaluated here.

Table 2. CPA EoS Molecular Parameters, Deviations for ρ and C_p, and Critical Properties for $[C_2C_1im][TCM]$ and $[4\text{-}C_4C_1py][TCM]$ ILs

	$[C_2C_1im][TCM]$		$[4\text{-}C_4C_1py][TCM]$	
IL	set 1	set 2	set 1	set 2
CPA EoS Parameters (Scheme 2B)				
p^0(443 K)/kPa	76.3	0.001	35.4	0.001
a_0/Pa m^6 mol^{-2}	0.4532	6.350	0.3707	8.320
$10^4 b$/m^3 mol^{-1}	1.685	1.804	2.080	2.245
c_1	5.985	1.504	6.816	1.362
$10^2\,\beta$	1.791	2.791	1.634	2.469
$10^4\varepsilon$/kJ mol^{-1}	1.293	1.507	1.770	1.535
ARD %				
ρ (0.1 MPa)	0.0950	0.981	0.0657	0.938
C_p	0.997	0.377	0.976	0.000100
Critical Properties[42]				
T_c/K	1149.4		1165.0	
p_c/MPa	2.460		1.785	
w	0.8509		0.9100	

Considering mixtures, a and b are calculated following the well-known vdW-1f mixing rules:

$$a = \sum_i \sum_j x_i x_j a_{ij}; \qquad a_{ij} = a_i a_j (1 - k_{ij}) \quad (8)$$

$$b = \sum_i x_i b_i \quad (9)$$

where k_{ij} are the binary interaction parameters. These are the only adjustable binary parameters applied in this work.

4. RESULTS AND DISCUSSION

4.1. CPA EoS Molecular Parameters for Tricyanomethanide-Based ILs. Both heat capacity and atmospheric density data were regressed by CPA EoS; the results are reported in Figure 1 (set 1). Density for both ILs was obtained from a recent work in which an exhaustive comparison with other literature sources was done.[39] On the other hand, heat capacities for $[C_2C_1im][TCM]$ were taken from the literature,[24] whereas this is the first work reporting heat capacities for $[4\text{-}C_4C_1py][TCM]$, collecting the new data in Table S1.

The regressed CPA EoS molecular parameters allow a good description of the properties with %ARD below 1% for ρ and C_p in the corresponding temperature ranges. The IL vapor pressures predicted using set 1 for the molecular parameters are of 76.3 and 35.4 kPa at 443.2 K (near thermal decomposition[22,24]) for $[C_2C_1im][TCM]$ and $[4\text{-}C_4C_1py][TCM]$ ILs, respectively. However, as reported by Emel'yanenko et al.[40] and Rocha et al.,[41] values ranging from 0.05 to 0.2 Pa are expected for

DOI: 10.1021/acs.iecr.8b03804
Ind. Eng. Chem. Res. 2018, 57, 14242−14253

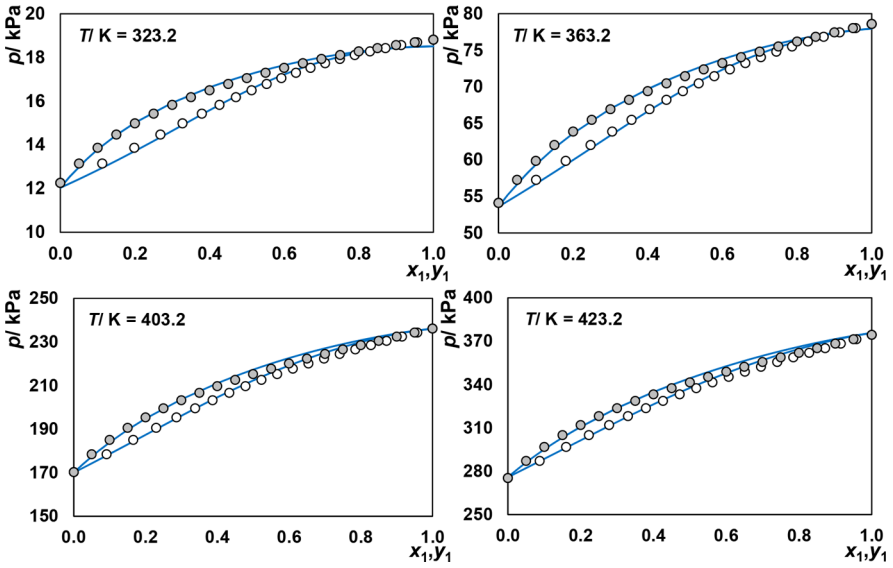

Figure 2. VLE data of *n*-heptane + toluene binary system. Symbols denote data from ref 42 and solid lines the CPA EoS with k_{12} reported in Table 3.

Table 3. CPA EoS Binary Interaction Parameters (k_{ij}) for the *n*-Heptane (1) + Toluene (2) + IL (3) System

		k_{13}		k_{23}	
T/K	k_{12}	[C_2C_1im][TCM]	[4-C_4C_1py][TCM]	[C_2C_1im][TCM]	[4-C_4C_1py][TCM]
323.2	0.013	0.000	0.040	−0.045	−0.040
363.2	0.010	0.010	0.045	−0.045	−0.035
403.2	0.007	0.020	0.055	−0.035	−0.020
423.2	0.004	0.020	0.060	−0.030	−0.010

imidazolium-based ILs near 450 K. Thus, the CPA EoS molecular parameters from set 1 will have an important impact on the VLLE description.

Therefore, aiming at obtaining a better description of the VLLE of the systems evaluated, a second regression of the ILs molecular parameters (set 2) was performed limiting the IL vapor pressure to be lower than 1 Pa, ensuring thus the nonvolatile character of the ILs in the CPA EoS modeling and keeping a reasonable description for density as detailed below. This approach lead to a deterioration of the density description at atmospheric pressure but improves the description of the C_p data. Nonetheless, the deviations found for density are analogous to those reported for CPA EoS in previous works.[38] Energy parameter completely conditions both vapor pressure and density dependency on temperature; hence, it is necessary to fulfill an adequate vapor pressure before improving density description. Both CPA EoS molecular parameter sets along with estimated critical properties taken from the literature[42] and average relative deviation (%ARD) obtained from the CPA EoS description of the ρ and C_p data are reported in Table 2. However, only those providing negligible vapor pressure were used in the phase equilibria description.

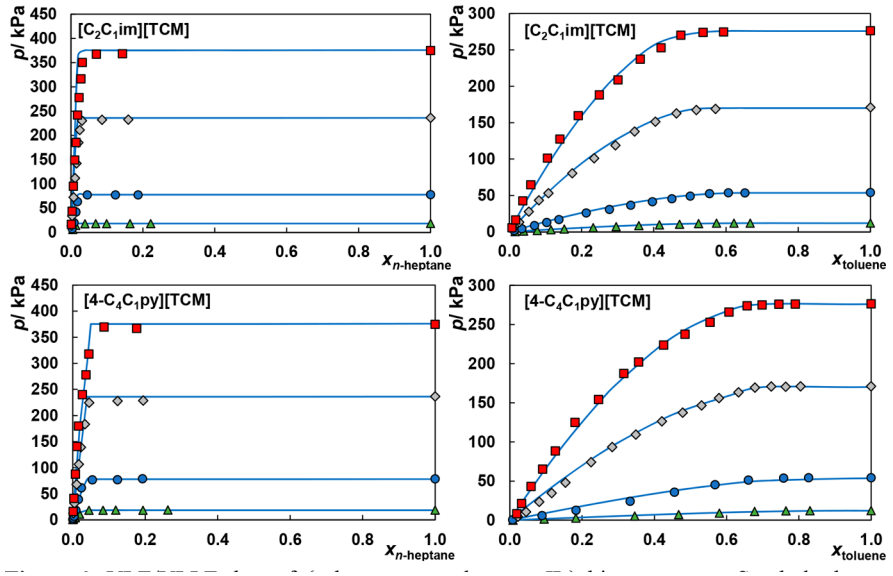

Figure 3. VLE/VLLE data of {*n*-heptane or toluene + IL} binary system. Symbols denote experimental data at △, 323.2 K; ○, 363.2 K; ◇, 403.2 K; and □, 423.2 K; and the solid lines the CPA EoS with k_{i3} listed in Table 3. {*n*-heptane or toluene + [4-C_4C_1py][TCM]} experimental data, at 323.2 and 363.2 K, were taken from ref 22.

DOI: 10.1021/acs.iecr.8b03804
Ind. Eng. Chem. Res. 2018, 57, 14242−14253

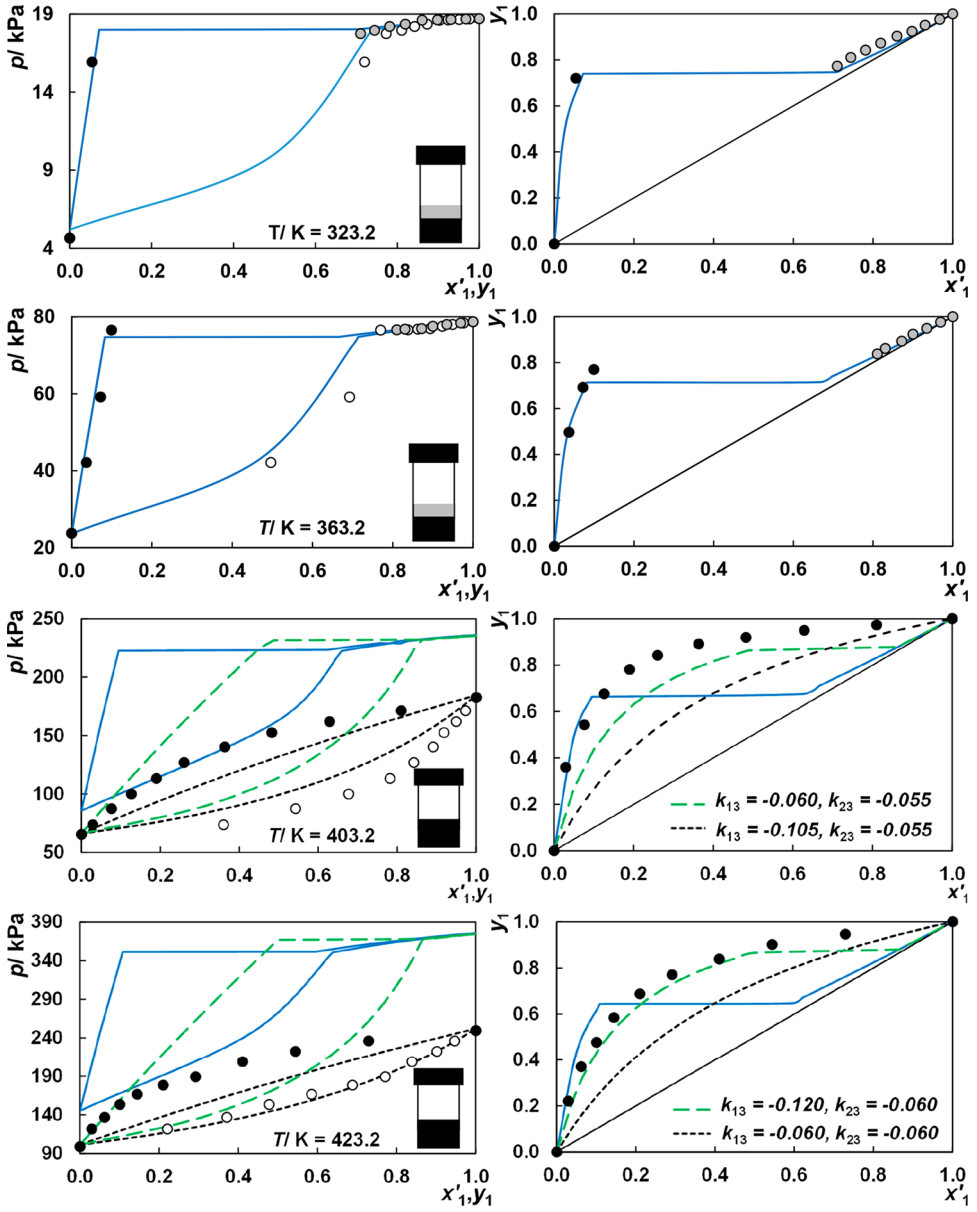

Figure 4. VLE $p-xy$ and $y-x$ diagrams for the *n*-heptane (1) + toluene (2) + $[C_2C_1im][TCM]$ (3) ternary system with S/F = 10. Symbols: black, IL-rich liquid phase; gray, hydrocarbon-rich liquid phase; and white, vapor phase. Lines: Solid represents the CPA EoS with k_{i3} reported in Table 3, and dashed denotes several scenarios with different k_{i3} values.

4.2. VLE and VLLE for Binary Systems Composed of *n*-Heptane, Toluene, and Tricyanomethanide-Based ILs: Experimental versus CPA EoS Description. The VLE for the *n*-heptane + toluene binary system taken from literature[42] was modeled with the CPA EoS for temperatures ranging from 323.2 to 423.2 K, as depicted in Figure 2. The results show the ability of CPA EoS to describe correctly the binary system within the studied temperature and composition ranges using k_{12} values with a small temperature dependency as reported in Table 3.

The VLE/VLLE values of the binary systems composed of *n*-heptane or toluene with $[C_2C_1im][TCM]$ and $[4\text{-}C_4C_1py]$-$[TCM]$ were determined in this work, at temperatures between 323 and 423 K, by HS-GC methodology, and the data are depicted in Figure 3 and reported in Tables S2 and S3.

The shape of the hydrocarbon + IL $p-x$ curves is well-known and consists of two different regions, VLE and VLLE. An increase in pressure is observed as the hydrocarbon mole fraction increases up to the maximum hydrocarbon solubility in the IL (VLE), whereas a VLLE region, with constant pressure, is observed for higher hydrocarbon concentrations. In the wide temperature range analyzed, the liquid−liquid region is weakly dependent on temperature, in line with the results of Hansmeier et al.[43] The CPA EoS was used for the experimental phase equilibria description of these binary systems, with the required binary interaction parameters reported in Table 3. CPA EoS correctly describes the *n*-heptane or toluene + IL systems with a small temperature-dependent binary interaction parameter.

4.3. VLE/VLLE for *n*-Heptane + Toluene + IL Ternary Systems: Experimental and CPA EoS Description. The VLE/VLLE was determined for *n*-heptane + toluene + IL ternary mixtures at 323.2, 363.2, 403.2, and 423.2 K. The hydrocarbons' binary mixture composition was studied within all composition ranges, whereas the solvent to feed ratio was evaluated from

DOI: 10.1021/acs.iecr.8b03804
Ind. Eng. Chem. Res. 2018, 57, 14242−14253

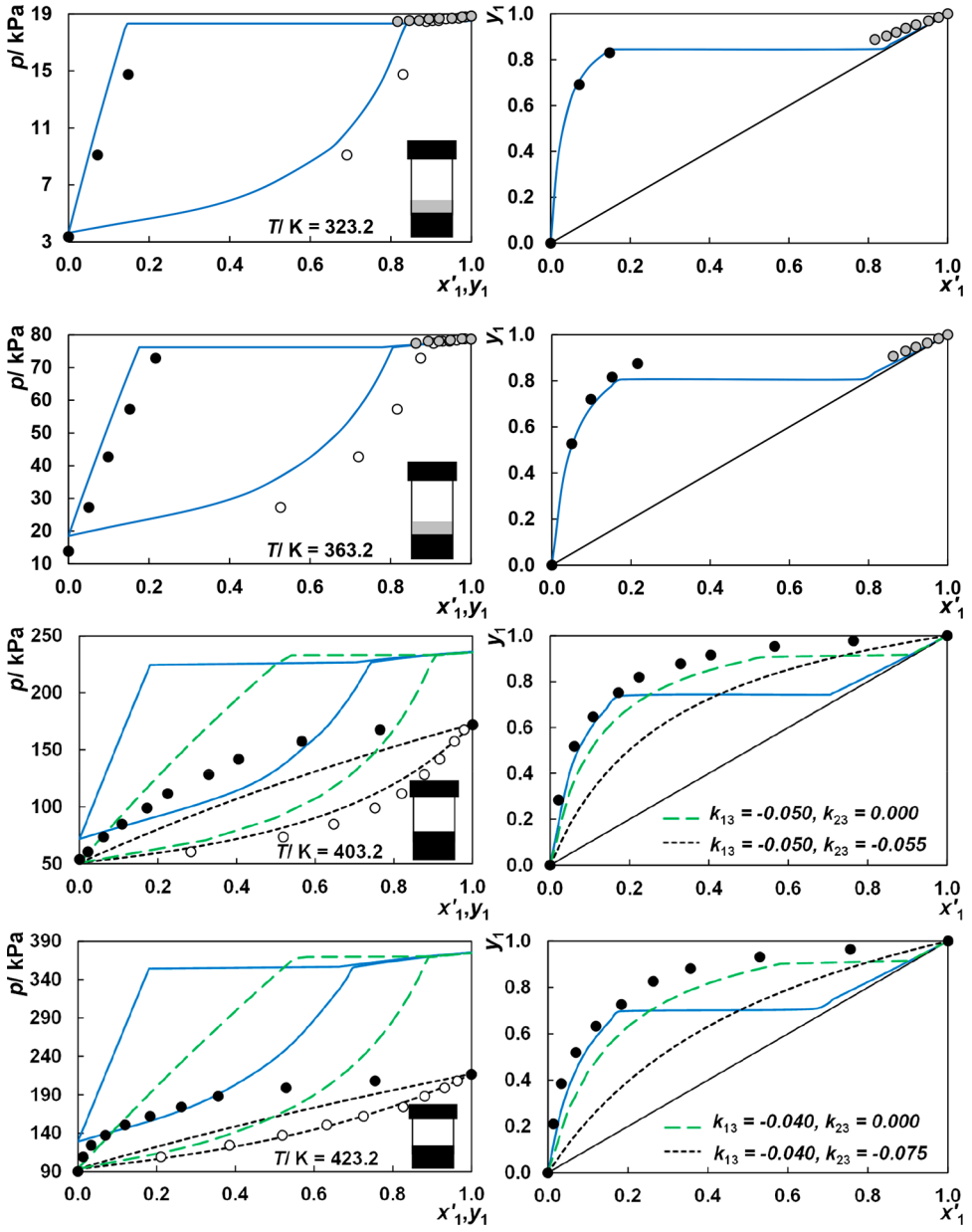

Figure 5. VLE $p-xy$ and $y-x$ diagrams for the *n*-heptane (1) + toluene (2) + [4-C_4C_1py][TCM] (3) ternary system with S/F = 10. Symbols: black, IL-rich liquid phase; gray, hydrocarbon-rich liquid phase; and white, vapor. Lines: Solid represents the CPA EoS wth k_{i3} from Table 3, and dashed denotes several scenarios with different k_{i3} values.

1 to 10, as this range covers that of interest for the envisioned separation.[21] The VLE/VLLE data for ternary systems are reported in Tables S4–S7.

4.3.1. VLE/VLLE Temperature Dependency for S/F = 10. As can be seen in Figures 4 and 5, two behaviors can be identified: for temperatures up to 363.2 K both VLLE and VLE regions are present, while only VLE is observed for the highest temperatures. Aiming at clarifying the phases present, a scheme is shown as the inset on the $p-xy$ diagrams where black and gray stand for the liquid phases and white for the gas phase. For temperatures up to 363 K, a homogeneous (VLE) region that increases with temperature is observed for *n*-heptane mole fractions below its solubility limit. The slope of the $p-xy$ diagram decreases as the temperature increases, showing a moderate negative impact in the *n*-heptane/toluene separation.

On the other hand, ternary phase diagrams, depicted in Figure 6, were selected to show the LLE region. As depicted, both ILs present a large immiscibility zone with a hydrocarbon-rich phase with negligible amounts of IL, and an IL-rich phase with a small amount of hydrocarbon, denoting the high capacity and selectivity of the studied ILs. As the temperature increases, the liquid–liquid region decreases mostly by increasing the amount of hydrocarbon in the IL-rich phase, while the hydrocarbon-rich phase remains free of IL.

As shown, the CPA EoS is able to provide an adequate description of the VLE/VLLE using the binary interaction parameters obtained from binary systems. Overall, the CPA EoS description of the $p-xy$ and ternary phase diagrams, at 323.2 and 363.2 K, is quite accurate with a small deviation around 3%. Higher deviations are observed, nonetheless, in the $p-xy$ diagrams for temperatures above 403.2 K. These deviations are

DOI: 10.1021/acs.iecr.8b03804
Ind. Eng. Chem. Res. 2018, 57, 14242–14253

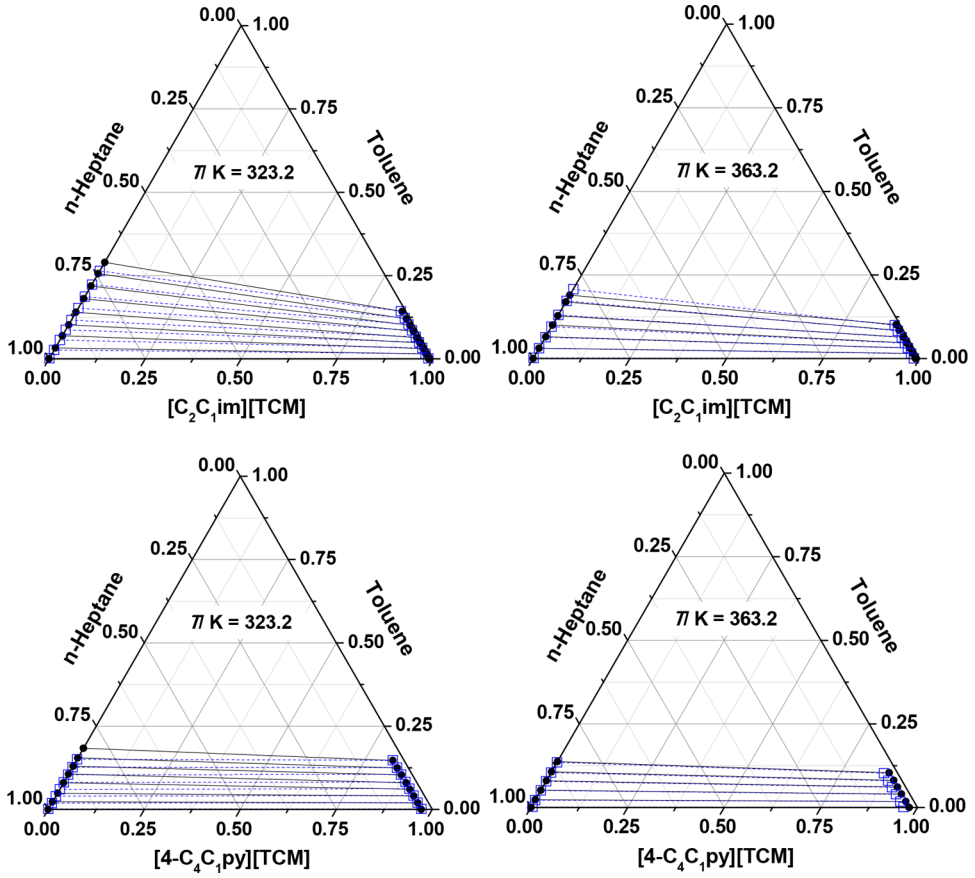

Figure 6. Ternary LLE diagrams from the VLLE data of *n*-heptane + toluene + IL ternary system with S/F = 10. Full symbols and solid lines denote experimental data, and empty squares and dashed lines are the CPA EoS.

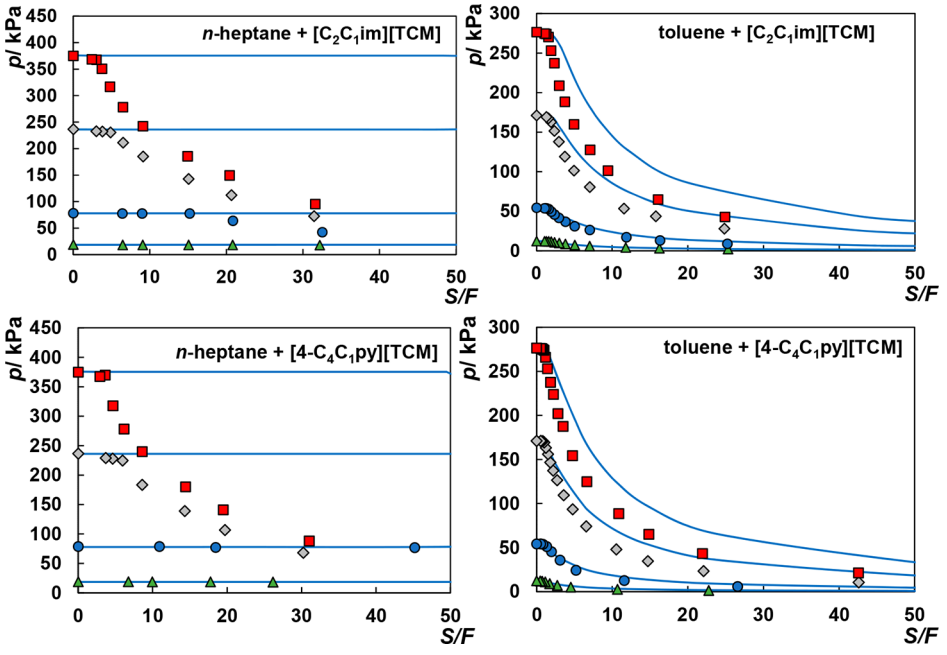

Figure 7. Pressure versus solvent to feed ratio (S/F) diagrams. Symbols denote experimental data at △, 323.2 K; ○, 363.2 K; ◇, 403.2 K; □, 423.2 K; and solid lines the CPA EoS with k_{ij} listed in Table 3. Experimental data for the {hydrocarbon + [4-C_4C_1py][TCM]} systems, at 323.2 and 363.2 K, were taken from ref 22.

related to the deterioration of the CPA EoS description with temperature, also observed in the binary systems. The relationship between pressure and S/F ratio, depicted in Figure 7, deteriorates with temperature, implying a pressure overestimation and poor description of the homogeneous phase behavior observed above 403.2 K, in the whole composition range. By contrast, the *y*−*x* diagram was properly described.

DOI: 10.1021/acs.iecr.8b03804
Ind. Eng. Chem. Res. 2018, 57, 14242−14253

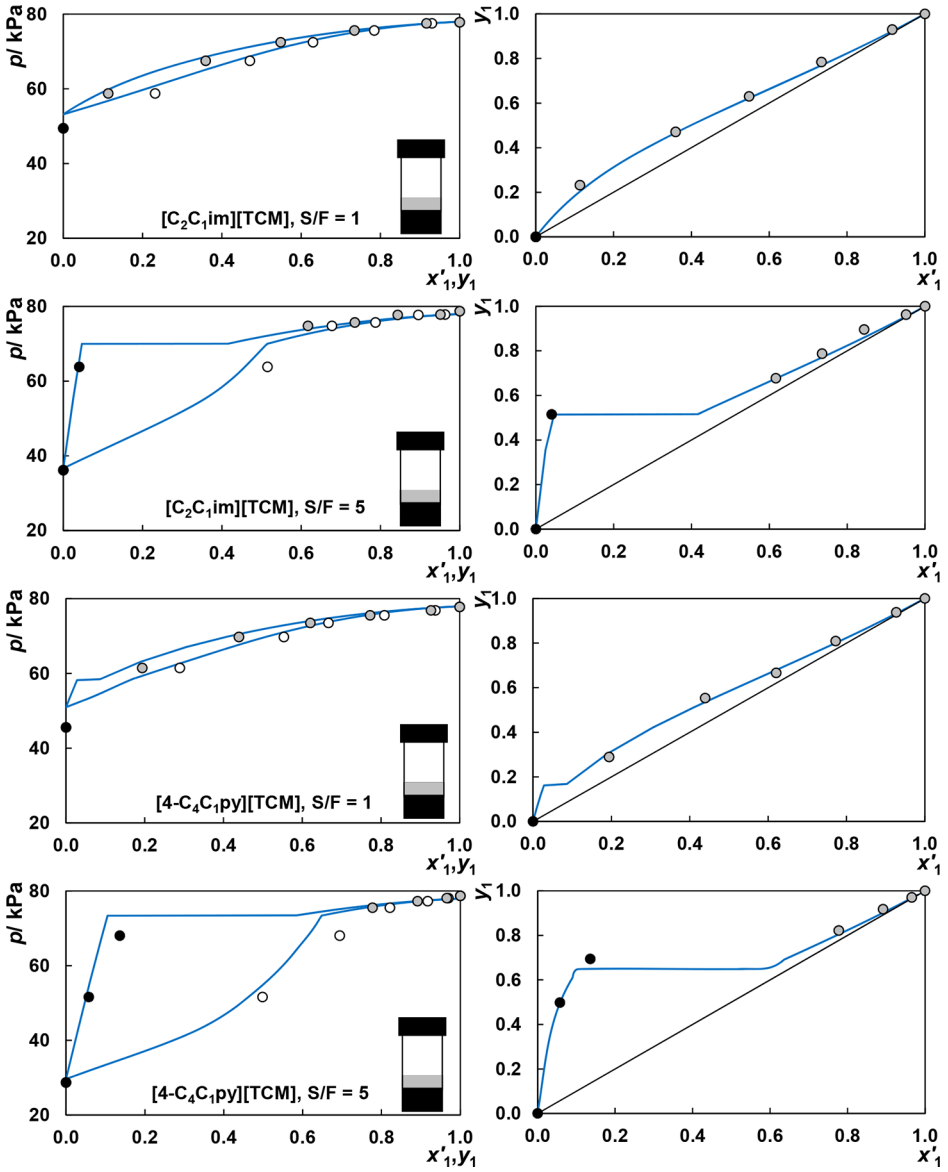

Figure 8. VLE $p-xy$ diagrams from the VLE/VLLE data of *n*-heptane (1) + toluene (2) + IL (3) ternary system at 363.2 K with S/F ratios of 1 and 5. Black symbols, IL-rich liquid phase; gray, IL-free liquid phase; and white, vapor phase. Solid lines represent the CPA EoS prediction.

Considering the temperature profile in an extractive distillation column, temperatures up to 403.2 K may be of interest only for the bottom steps, which are related to toluene high concentration region. In this context, a slight modification of the k_{23}, to properly describe the toluene (2) + IL (3) mixture composition, and the k_{13}, to provide a compensation in the description between the equilibrium pressures and the vapor−liquid compositions (long-dashed lines), allows one to obtain an adequate description of the VLE and VLLE and thus a better process simulation (see Figures 4 and 5).

4.3.2. VLE/VLLE Description as a Function of S/F Ratio at 363.2 K. To assess the suitability of the EoS for a wide range of conditions, other S/F ratios were evaluated. VLLE data were determined for S/F ratios of 1 and 5, at 363.2 K. The experimental results are plotted in Figure 8 (VLE, $p-xy$ and $y-x$ diagrams) and Figure 9 (ternary phase diagrams) together with a CPA EoS description using only the binary interaction parameters reported in Table 3. As can be seen, the CPA EoS is able to provide a very good predictive description of the phase equilibria.

Although the dependency of binary interaction parameters with the S/F ratio was evaluated only for ternary systems at 363.2 K, this is implicit in the binary systems for all of the temperatures evaluated. Thus, one can claim that CPA EoS is suitable up to an S/F ratio of 10 and temperatures ranging from 323.2 to 423.2 K. Further remarks regarding the robustness of the model for its practical implementation in a process simulator are given below (section 4.4) through the analyses of the toluene/*n*-heptane relative volatilities in the presence of the ILs and ILs' extractive properties.

4.4. Analysis of *n*-Heptane/Toluene Relative Volatility and ILs' Extractive Properties. The tricyanomethanide-based ILs' suitability for the *n*-heptane/toluene separation by extractive distillation was shown in the phase equilibria analysis. However, the IL effectiveness is quantitatively given by the *n*-heptane (1) relative volatility to toluene (2), which can be calculated from the experimental data as follows:

$$\alpha_{12} = \frac{K_1}{K_2} = \frac{y_1/x_1}{y_2/x_2} \tag{10}$$

DOI: 10.1021/acs.iecr.8b03804
Ind. Eng. Chem. Res. 2018, 57, 14242−14253

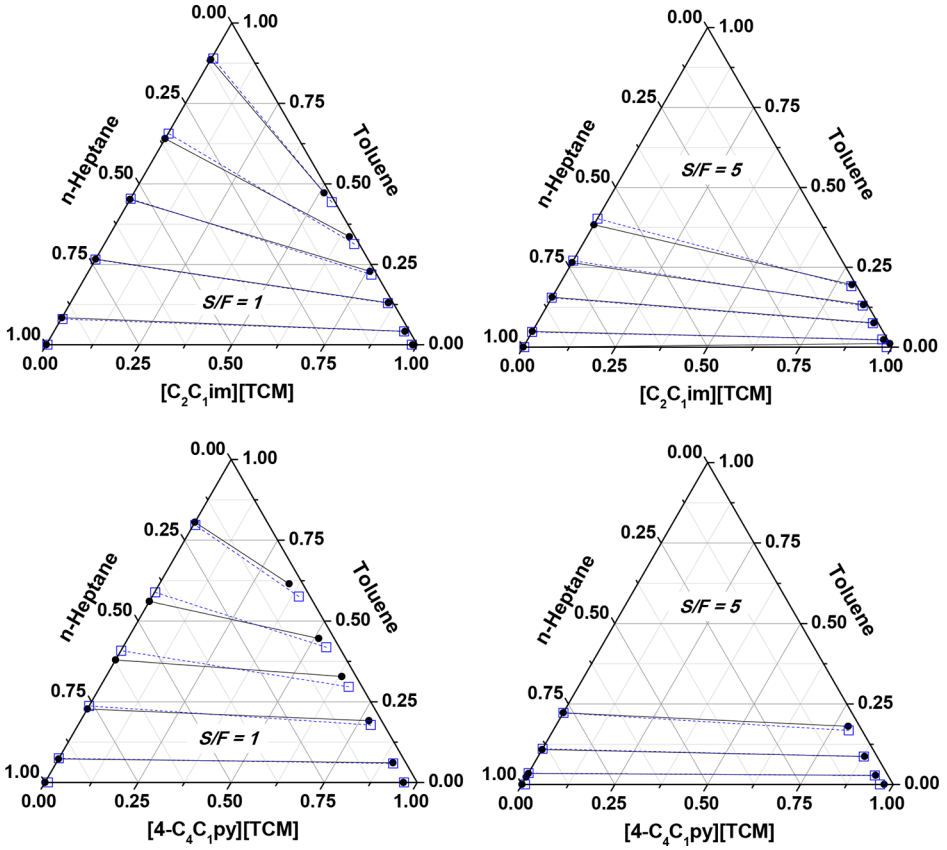

Figure 9. Ternary LLE phase diagrams of the *n*-heptane (1) + toluene (2) + IL (3) ternary systems at 363.2 K with S/F ratios of 1 and 5. Full symbols and solid lines denote experimental data, and empty squares and dashed lines are the CPA EoS.

where K is the K-value, and y_i and x_i denote the vapor and liquid phase mole fractions of component i, respectively. The *n*-heptane/toluene relative volatility is determined along with the experimental VLE/VLLE data reported in Tables S3−S12 and depicted in Figure 10. As can be seen, two trends can be identified: up to 363 K *n*-heptane/toluene relative volatility remains, within experimental uncertainty, almost constant within the homogeneous region, followed by an asymptotic decrease as *n*-heptane mole fraction increases in the heterogeneous region. For temperatures higher than 363 K, the *n*-heptane/toluene relative volatility slightly decreases with increasing *n*-heptane mole fraction. Furthermore, [C_2C_1im][TCM] presents a higher toluene/*n*-heptane selectivity, enhancing thus higher separation factors in the homogeneous region as discussed in a previous work;[44] however, [4-C_4C_1py][TCM] stands as a better mass agent in the heterogeneous regions due to its higher toluene distribution ratios as previously reported.[21] The CPA EoS is able to describe the relative volatilities and to mimic the reported effects, standing as an adequate EoS to model these systems.

A comparison between calculated extractive properties from experimental data and CPA EoS is presented in Figure 11. Hydrocarbon distribution ratios (D_i) and toluene (2)/*n*-heptane (1) selectivity ($S_{2,1}$) were calculated as follows:

$$D_i = \frac{w_i^{II}}{w_i^{I}} \tag{11}$$

$$S_{2,1} = \frac{D_2}{D_1} \tag{12}$$

where w_i is the mass fraction of component i, and superscripts I and II refer to IL-free liquid phase and IL-rich liquid phase, respectively. Toluene/*n*-heptane selectivity decreases, and toluene distribution ratio is hardly affected by toluene mole fraction. Regarding S/F ratio and T effects, it is found that its impact on the toluene/*n*-heptane selectivity is low, whereas it has almost no influence on the toluene distribution ratios. Although is widely accepted that both temperature and S/F ratio negatively impact the extractive properties,[8,43,45] Hansmeier et al.[43] reported also that temperature hardly affects extractive properties in the toluene separation from *n*-heptane by liquid−liquid extraction using cyano-based ILs in the temperature range of 313.2−348.2 K. Furthermore, Larriba et al.[8] and Navarro et al.[45,46] showed that both temperature and S/F ratio had a low impact on the extractive properties using cyano-based ILs. Considering literature background, extractive properties calculated in this work are consistent. Moreover, CPA EoS provides a good description for both extractive properties, even considering the high toluene/*n*-heptane selectivity values for both ILs. In this context, the deviations observed for toluene/*n*-heptane selectivity are admissible, and, keeping in mind a vapor−liquid separation perspective, they will not impact on the extractive distillation column design.

5. CONCLUSIONS

New VLE/VLLE data for the binary and ternary systems composed of *n*-heptane, toluene, and two ILs, [C_2C_1im][TCM] and [4-C_4C_1py][TCM], were measured in a wide range of temperatures and S/F ratios aiming at evaluation of the selected ILs as solvents for the toluene/*n*-heptane extractive distillation.

DOI: 10.1021/acs.iecr.8b03804
Ind. Eng. Chem. Res. 2018, 57, 14242−14253

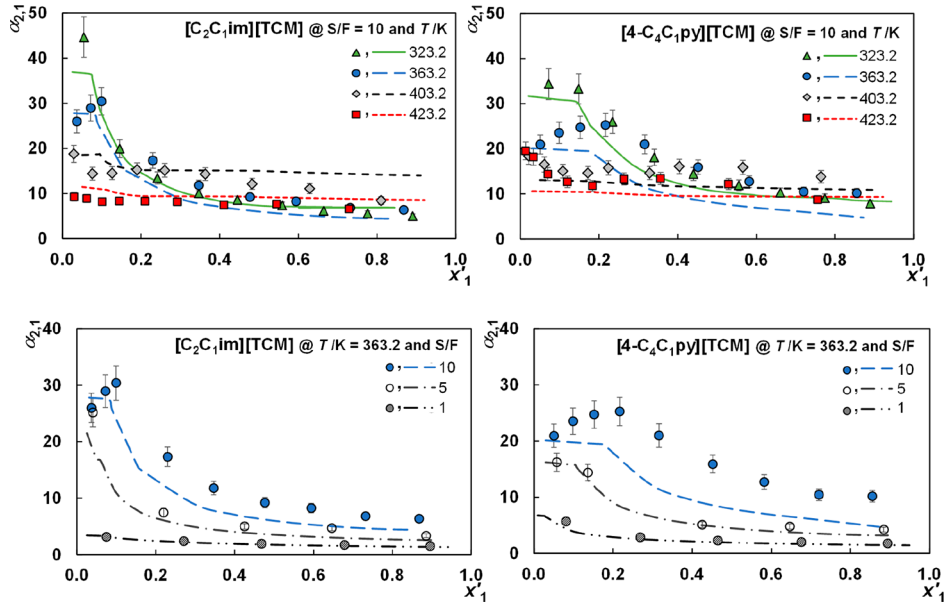

Figure 10. Values of *n*-heptane/toluene relative volatility calculated from experimental (symbol) and CPA EoS (lines) for *n*-heptane (1) + toluene (2) + IL (3) ternary systems as a function of the free-IL *n*-heptane mole fraction, x'_1, in overall liquid, temperature, and S/F ratio.

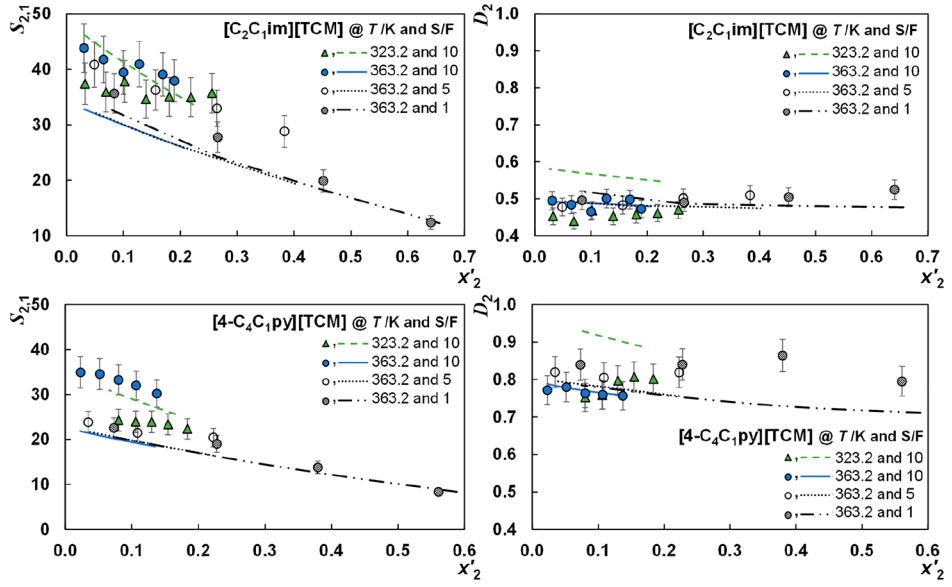

Figure 11. Values of toluene/*n*-heptane selectivity and toluene distribution ratio calculated from the LLE data and CPA EoS for *n*-heptane (1) + toluene (2) + IL (3) ternary systems as a function of the free-IL toluene mole fraction, x'_2, in overall liquid, temperature, and S/F ratio.

A VLLE region was observed at low temperatures and high *n*-heptane concentrations where the IL is not capable of solubilizing the whole *n*-heptane present in the liquid phase. The results allow one to establish the adequate conditions, homogeneous or heterogeneous phases, for the extractive distillation.

CPA EoS was used to describe the experimental data, and new molecular parameters for the studied ILs, defined as associating molecules with scheme 2B, were proposed. CPA EoS was able to simultaneously describe phase equilibria and the density and C_p of the pure compounds. Temperature-dependent binary interaction parameters were required to accurately describe both VLLE and VLE regions in a wide range of temperatures (323.2−423.2 K) and S/F ratios (1−10). The proposed molecular parameters, molecular scheme, and binary interaction parameters were able to correctly describe the toluene/*n*-heptane relative volatilities and extractive properties of the ILs.

The high separation effectiveness using extractive distillation with tricyanomethanide-based ILs in the whole range of conditions has shown the potential of the selected technology and solvents. The high benzene concentration in real gasoline and naphtha will smooth operating temperatures given in this work to operate under homogeneous conditions, whereas heterogeneous extractive distillation does not seem to be an important drawback as separation factors are high enough to ensure the separation, although the column would have certain inefficient volumes.

To further explore the extractive distillation with ILs to separate aromatics from aliphatics in other characteristic and more complex models, the HS-GC and CPA EoS are shown to be a good combination of an experimental-modeling strategy.

DOI: 10.1021/acs.iecr.8b03804
Ind. Eng. Chem. Res. 2018, 57, 14242−14253

■ ASSOCIATED CONTENT

Supporting Information

The Supporting Information is available free of charge on the ACS Publications website at DOI: 10.1021/acs.iecr.8b03804.

Heat capacity of [4-C_4C_1py][TCM] in Table S1, binary vapor−liquid and vapor−liquid−liquid equilibria in Tables S2 and S3, and ternary vapor−liquid and vapor−liquid−liquid equilibria in Tables S4−S7 (PDF)

■ AUTHOR INFORMATION

Corresponding Author

*E-mail: pntejedor@ua.pt.

ORCID

Pablo Navarro: 0000-0002-0017-3898
André M. Palma: 0000-0002-5580-6883
Julián García: 0000-0003-1386-4003
João A. P. Coutinho: 0000-0002-3841-743X
Pedro J. Carvalho: 0000-0002-1943-0006

Funding

This work was developed in the scope of the project CICECO-Aveiro Institute of Materials, POCI-01-0145-FEDER-007679 (ref. FCT UID/CTM/50011/2013) funded by FEDER through COMPETE2020-Programa Operacional Competitividade e Internacionalização (POCI) and by national funds through FCT-Fundação para a Ciência e a Tecnologia. We are also grateful to Ministerio de Economía y Competitividad (MINECO) of Spain and Comunidad Autónoma de Madrid for financial support of projects CTQ2017-85340-R and S2013/MAE-2800, respectively. P.N. and P.J.C. also thank FCT for awarding their postdoctoral grant (SFRH/BPD/117084/2016) and contract under the Investigator FCT 2015 (IF/00758/2015), respectively. N.D.-M. also thanks MINECO for awarding her an FPI grant (BES-2015-072855). M.L. thanks Ministerio de Eduación, Cultura y Deporte of Spain, for awarding him a José Castillejo postdoctoral mobility grant (CAS17/00018). We thank Infochem-KBC because the Multiflash program was applied for the CPA EoS calculations.

Notes

The authors declare no competing financial interest.

■ REFERENCES

(1) Franck, H. G.; Staldelhofer, J. W. *Industrial Aromatic Chemistry*; Springer−Verlag: Berlin, 1988.

(2) Canales, R. I.; Brennecke, J. F. Comparison of ionic liquids to conventional organic solvents for extraction of aromatics from aliphatics. *J. Chem. Eng. Data* **2016**, *61*, 1685−1699.

(3) Domanska, U.; Wlazlo, M. Effect of the cation and anion of the ionic liquid on desulfurization of model fuels. *Fuel* **2014**, *134*, 114−125.

(4) Rogers, R. D.; Seddon, K. R. Ionic liquids-solvents of the future? *Science* **2003**, *302*, 792−793.

(5) Cao, Y.; Mu, T. Comprehensive Investigation on the Thermal Stability of 66 Ionic Liquids by Thermogravimetric Analysis. *Ind. Eng. Chem. Res.* **2014**, *53*, 8651−8664.

(6) Larriba, M.; Navarro, P.; García, J.; Rodríguez, F. Liquid−Liquid Extraction of BTEX from Reformer Gasoline Using Binary Mixtures of [4empy][Tf_2N] and [emim][DCA] Ionic Liquids. *Energy Fuels* **2014**, *28*, 6666−6676.

(7) Larriba, M.; Navarro, P.; González, E. J.; García, J.; Rodríguez, F. Separation of BTEX from a naphtha feed to ethylene crackers using a binary mixture of [4empy][Tf_2N] and [emim][DCA] ionic liquids. *Sep. Purif. Technol.* **2015**, *144*, 54−62.

(8) Larriba, M.; Navarro, P.; González, E. J.; García, J.; Rodríguez, F. Dearomatization of pyrolysis gasolines from mild and severe cracking by liquid−liquid extraction using a binary mixture of [4empy][Tf_2N] and [emim][DCA] ionic liquids. *Fuel Process. Technol.* **2015**, *137*, 269−282.

(9) Navarro, P.; Larriba, M.; García, J.; Rodríguez, F. Design of the Hydrocarbon Recovery Section from the Extract Stream of the Aromatic Separation from Reformer and Pyrolysis Gasolines Using a Binary Mixture of [4empy][Tf_2N] + [emim][DCA] Ionic Liquids. *Energy Fuels* **2017**, *31*, 1035−1043.

(10) Navarro, P.; Larriba, M.; García, J.; Rodríguez, F. Design of the recovery section of the extracted aromatics in the separation of BTEX from naphtha feed to ethylene crackers using [4empy][Tf_2N] and [emim][DCA] mixed ionic liquids as solvent. *Sep. Purif. Technol.* **2017**, *180*, 149−156.

(11) Lei, Z.; Li, C.; Chen, B. Extractive Distillation: A Review. *Sep. Purif. Rev.* **2003**, *32*, 121−213.

(12) Lei, Z.; Dai, C.; Zhu, J.; Chen, B. Extractive Distillation with Ionic Liquids: A Review. *AIChE J.* **2014**, *60*, 3312−3329.

(13) Rodríguez-Cabo, B.; Rodríguez, H.; Rodil, E.; Arce, A.; Soto, A. Extractive and oxidative-extractive desulfuration of fuels with ionic liquids. *Fuel* **2014**, *117*, 882−889.

(14) Paduszynski, K.; Królikowski, M.; Zawadzki, M.; Orzet, P. Computer-Aided Molecular Design of New Task-Specific Ionic Liquids for Extractive Desulfurization of Gasoline. *ACS Sustainable Chem. Eng.* **2017**, *5*, 9032−9042.

(15) Jongmans, M. T. G.; Schuur, B.; de Haan, A. B. Ionic Liquid Screening for Ethylbenzene/Styrene Separation by Extractive Distillation. *Ind. Eng. Chem. Res.* **2011**, *50*, 10800−10810.

(16) Díaz, I.; Palomar, J.; Rodríguez, M.; de Riva, J.; Ferro, V.; González, E. J. Ionic liquids as entrainers for the separation of aromatic−aliphatic hydrocarbon mixtures by extractive distillation. *Chem. Eng. Res. Des.* **2016**, *115*, 382−393.

(17) Dong, Y.; Dai, C.; Lei, Z. Extractive distillation of methylal/methanol mixture using the mixture of dimethylformamide (DMF) and ionic liquid as entrainers. *Fuel* **2018**, *216*, 503−512.

(18) Kulajanpeng, K.; Suriyapraphadilok, U.; Goni, R. Systematic screening methodology and energy efficient design of ionic liquid-based separation processes. *J. Cleaner Prod.* **2016**, *111*, 93−107.

(19) Anjan, S. T. Ionic Liquid for Aromatic Extraction: Are They Ready? *Chem. Eng. Prog.* **2006**, *102*, 30−39.

(20) de Riva, J.; Ferro, V. R.; Moreno, D.; Díaz, I.; Palomar, J. Aspen Plus supported conceptual design of the aromatic−aliphatic separation from low aromatic content naphtha using 4-methyl-N-butylpyridinium tetrafluoroborate ionic liquid. *Fuel Process. Technol.* **2016**, *146*, 29−38.

(21) Navarro, P.; Larriba, M.; Delgado-Mellado, N.; Ayuso, M.; Romero, M.; García, J.; Rodríguez, F. Experimental screening towards developing ionic liquid-based extractive distillation in the dearomatization of refinery streams. *Sep. Purif. Technol.* **2018**, *201*, 268−275.

(22) Larriba, M.; Navarro, P.; Delgado-Mellado, N.; Stanisci, V.; García, J.; Rodríguez, F. Separation of aromatics from n-alkanes using tricyanomethanide-based ionic liquids, Liquid-liquid extraction, vapor-liquid separation, and thermophysical characterization. *J. Mol. Liq.* **2016**, *223*, 880−889.

(23) Larriba, M.; Navarro, P.; García, J.; Rodríguez, F. Liquid-liquid extraction of toluene from heptane using [emim][DCA], [bmim]-[DCA], and [emim][TCM] ionic liquids. *Ind. Eng. Chem. Res.* **2013**, *52*, 2714−2720.

(24) Navarro, P.; Larriba, M.; Rojo, E.; García, J.; Rodríguez, F. Thermal properties of cyano-based ionic liquids. *J. Chem. Eng. Data* **2013**, *58*, 2187−2193.

(25) Navarro, P.; Larriba, M.; García, J.; González, E. J.; Rodríguez, F. Vapor-liquid equilibria of {n-heptane + toluene + [emim][DCA]} system using headspace gas chromatography. *Fluid Phase Equilib.* **2015**, *387*, 209−216.

(26) Perry, R. H.; Green, D. W.; Maloney, J. O. *Perry's Chemical Engineers' Handbook*; McGraw−Hill: New York, 1999.

(27) Kontogeorgis, G. M.; Michelsen, M. L.; Folas, G. K.; Derawi, S.; von Solms, N.; Stenby, E. H. Ten Years with the CPA Cubic-Plus-Association;, Equation of State. Part 1. Pure Compounds and Self-Associating Systems. *Ind. Eng. Chem. Res.* **2006**, *45*, 4855−4868.

DOI: 10.1021/acs.iecr.8b03804
Ind. Eng. Chem. Res. 2018, 57, 14242−14253

(28) Kontogeorgis, G. M.; Michelsen, M. L.; Folas, G. K.; Derawi, S.; von Solms, N.; Stenby, E. H. Ten Years with the CPA Cubic-Plus-Association;, Equation of State. Part 2. Cross-Associating and Multicomponent Systems. *Ind. Eng. Chem. Res.* **2006**, *45*, 4869−4878.
(29) Soave, G. Equilibrium constants from a modified Redlich-Kwong equation of state. *Chem. Eng. Sci.* **1972**, *27*, 1197−1203.
(30) Redlich, O.; Kwong, J. N. S. On the Thermodynamics of Solutions. V. An Equation of State. Fugacities of Gaseous Solutions. *Chem. Rev.* **1949**, *44*, 233−244.
(31) Voutsas, E. C.; Yakoumis, I. V.; Tassios, D. P. Prediction of phase equilibria in water/alcohol/alkane systems. *Fluid Phase Equilib.* **1999**, *160*, 151−163.
(32) Michelsen, M. L.; Hendriks, E. M. Physical properties from association models. *Fluid Phase Equilib.* **2001**, *180*, 165−174.
(33) Wu, J. Z.; Prausnitz, J. M. Phase Equilibria for Systems Containing Hydrocarbons, Water, and Salt, An Extended Peng−Robinson Equation of State. *Ind. Eng. Chem. Res.* **1998**, *37*, 1634−1643.
(34) Kontogeorgis, G. M.; Folas, G. K. *Thermodynamic Models for Industrial Applications - From Classical and Advanced Mixing Rules to Association Theories*; John Wiley & Sons: Hoboken, NJ, 2010.
(35) Huang, S. H.; Radosz, M. Equation of state for small, large, polydisperse, and associating molecules. *Ind. Eng. Chem. Res.* **1990**, *29*, 2284−2294.
(36) Pereira, L. M. C.; Oliveira, M. B.; Llovell, F.; Vega, L. F.; Coutinho, J. A. P. Assessing the N_2O/CO_2 high pressure separation using ionic liquids with the soft-SAFT EoS. *J. Supercrit. Fluids* **2014**, *92*, 231−241.
(37) Oliveira, M. B.; Llovell, F.; Coutinho, J. A. P.; Vega, L. F. Modeling the [NTf_2] Pyridinium Ionic Liquids Family and Their Mixtures with the Soft Statistical Associating Fluid Theory Equation of State. *J. Phys. Chem. B* **2012**, *116*, 9089−9100.
(38) Maia, F. M.; Tsivintzelis, I.; Rodríguez, O.; Macedo, E. A.; Kontogeorgis, G. M. Equation of state modelling of systems with ionic liquids: Literature review and application with the Cubic Plus Association (CPA) model. *Fluid Phase Equilib.* **2012**, *332*, 128−143.
(39) Navarro, P.; Palma, A. M.; García, J.; Rodríguez, F.; Coutinho, J. A. P.; Carvalho, P. J. High pressure density of tricyanomethanide-based ionic liquids: experimental and PC-SAFT modelling. *J. Chem. Thermodyn.*, submitted.
(40) Emel'yanenko, V. N.; Verevkin, S. P.; Heitz, A. The Gaseous Enthalpy of Formation of the Ionic Liquid 1-Butyl-3-methylimidazolium Dicyanamide from Combustion Calorimetry, Vapor Pressure Measurements, and Ab Initio Calculations. *J. Am. Chem. Soc.* **2007**, *129*, 3930−3937.
(41) Rocha, M. A. A.; Lima, C.R.F.A.C.; Gomes, L. R.; Schröder, B.; Coutinho, J. A. P.; Marrucho, I. M.; Esperança, J. M. S. S.; Rebelo, L. P. N.; Shimizu, K.; Canongia Lopes, J. N.; Santos, L.N.M.B.F. High-Accuracy Vapor Pressure Data of the Extended [CnC1im][Ntf2] Ionic Liquid Series, Trend Changes and Structural Shift. *J. Phys. Chem. B* **2011**, *115*, 10919−10926.
(42) Valderrama, J. O.; Forero, L. A.; Rojas, R. E. Critical Properties and Normal Boiling Temperature of Ionic Liquids. Update and a New Consistency Test. *Ind. Eng. Chem. Res.* **2012**, *51*, 7838−7844.
(43) *Aspen Plus Version 7.1, Database*; Aspen Technology, 2004.
(44) Hansmeier, A. R.; Ruiz, M. M.; Meindersma, G. W.; de Haan, A. B. Liquid-Liquid Equilibria for the Three Ternary Systems 3-Methyl-N-butylpyridinium Dicyanamide + Toluene + Heptane), 1-Butyl-3-methylimidazolium Dicyanamide + Toluene + Heptane, and 1-Butyl-3-methylimidazolium Thiocyanate + Toluene + Heptane at T = 313.15 and 348.15 K and p = 0.1 MPa. *J. Chem. Eng. Data* **2010**, *55*, 708−713.
(45) Navarro, P.; Larriba, M.; González, E. J.; García, J.; Rodríguez, F. Selective recovery of aliphatics from aromatics in the presence of the {[4empy][Tf_2N] + [emim][DCA]} ionic liquid mixture. *J. Chem. Thermodyn.* **2016**, *96*, 134−142.
(46) Navarro, P.; Larriba, M.; Delgado-Mellado, N.; Sánchez-Migallón, P.; García, J.; Rodríguez, F. Extraction and recovery process to selectively separate aromatics from naphtha feed to ethylene crackers using 1-ethyl-3-methylimidazolium thiocyanate ionic liquid. *Chem. Eng. Res. Des.* **2017**, *120*, 102−112.

DOI: 10.1021/acs.iecr.8b03804
Ind. Eng. Chem. Res. 2018, 57, 14242−14253